HOT 130 UNDAR% LAYERS IN SYMBIOTIC BINARIES AX PERSEI AND CI CYGNI

PATRICK GODON

NASA/JET PROPULS1ON LABORATORY
CALIFORNIA INSTITUTE OF 1'ECHN0L0G%
4800 OAK GROVE DR. MS 238-332
PASADENA, CA 91109

EMAIL: GODON@ II ERCA. JPL. NASA.GOV

1. INTRODUCTION

Symbiotic systems are long period binaries in which a white dwarf usually accretes material from the wind of a red giant companion. Accretion in these systems, however, might also occur when a very evolved red giant overflows its Roch lobe. In this case the stream of mat ter flows beyond the first Lagrangian point and forms an accret ion disc around the accreting white dwarf. In the symbiotic systems AX Per and CI Cyg, the accreting secondary is yet a solar-type main-sequence star rather than a hot white dwarf (Kenyon et al. 1991; Mikołajewska & Kenyon 1992).

In CI Cyg, Kenyon et al. (1 991) derive a hot component temperature of 125 x 103K. They estimate $R_* \approx$ 0.2- $0.4 R_\odot$ and $M_* \approx 0.5 M_\odot$ for the accreting star, with M $\approx$ 1 --3 x $10^{-5} M_\odot/y$ during quiescence and M up to $10^{-3} M_\odot/y$ during outburst. For AX Per, Mikołajewska & Kenyon (1 992) find $T \approx$ 125- $145 \times 10^3 K$ for the hot component, while $R_* \approx 0.3 R_\odot$ and $M_* \approx 0.4 M_\odot$. They estimate M $\approx$ 1.5- 3 x $10^{-5} M_\odot/y$ during quiescence and $\dot{M} \approx$ 4 x $10^{-4} M_\odot/y$ during outburst. The radius R_* and mass M_* estimates are based on the investigation of Kenyon et al. (1 991), who avoid to treat the complex proper ties of the boundary layers by assuming that it can be approximated as a thin ring with a radial thickness $\delta R/R \approx v_s/v_K$ (Kenyon & Hartmann 1990, v_s and v_K are the ***sound*** and the Keplerian velocity respectively). In this picture, the energy dissipated in the dynamical boundary layer (of radial extend δ_{BL}) is emitted from a larger region (the thermal boundary layer) of extend $\delta R \approx H_{BL} > \delta_{BL}$ (H_{BL}, the disc thickness in the inner region of the disc, Pringle 19'77). As M increases from 10^{-5} up to few $10^{-4} M_\odot/y$, the vertical thickness of the disc is believed to increase from 0.01 - $0.05 R_*$ up to $0.3 R_*$, and therefore the boundary layer is believed to cool (K enyon et al. 1991).

In both systems the optical luminosity (which originates from the disc) increases from $\approx 10^2 L_\odot$ (during quiescence) up to $\approx 10^4 L_\odot$ (at maximum outburst). However, the *H* eII emission lines present during quiescence (originating from the " hot component" - the boundary layer) are not observed at maximum, which means that the effective temperature in the boundary layer probably falls below 60, *000K*. In addition, the lack of emission lines with moderate ionization potentials indicates that it can be as low as 10,000 – 20,0001< at maximum.

Recent one-dimensional boundary layer calculations (1 'opham et al. 1993; Lioure & Le Contel 1994; Popham & Narayan 1995; Godon 1995a,b; Godon, Regev & Shaviv 1995) have shown indeed that the energy dissipated in the dynamical boundary layer (region of nigh shear, due **to** the gradient of the angular velocity) is emitted from a much wider region (the thermal boundary layer), therefore leading to rather cool 1 oundary layers (see also section 2). In these calculations the ter-in for the radial diffusion of energy in the disc is essential to reproduce the results: the energy dissipated in the dynamical boundary layer is radiated radial] y outward, However, all the above numerical calculations were carried out for accretion discs around white dwarfs (Popham & Narayan 1995; Godon 1995a; Godon

et al. 1995) and around pre-main sequence stars (Popham et al. 1 993; Lioure & Le Contel 1994; Godon 1995b). So far, no boundary layer calculations have been performed around main-sequence stars with $R_* \approx$ 0.2 – 0.4, $M_* \approx 0.5 M_\odot$ and $\dot{M} \approx 10^{-5}$ – 4 x $10^{-4} M_\odot/y$.

The pm-pose of the present work is to provide, for the fi st time, boundary layer calculations for symbiotic stars, and to answer the question whether boundary layer models can explain the observed behaviour of the hot component in out bursts of symbiotic stars.

in section **2** the numerical modeling of the boundary layer region is reviewed. The numerical results for AX Per and CI Cyg are presented in section 3 and discussed in section 4.

2. MODELING ACCRETION DISCS BOUNDARY LAYERS

2.1 Equations and assumptions

The equations arc written and solved in cylindrical coordinates (r,+, z). Axisymmetry is assumed around the z-axis, and the equations arc vertically integrated. The remaining equations arc, therefore, one dimensional (in r). They include the gravity of the accreting star, viscosity and radiative transfer treated in t] ic diffusion approximation. Radiation pressure is further taken into account in the equation of state. The medium is assumed to bc optically thick. The exact form of the equations and the physical assumptions have been widely described in Godon (1995a,b), and Godon et al. (1995). Therefore, only a brief description of the assumptions arc given here. For more details the reader is referred to the above references.

At the inner boundary of the computational domain, the accreting star rotates at constant angular velocity ($\Omega_* = 0.1\ \Omega_K(R_*)$) and a constant inflow of matter (Al) flows into the stellar surface. A non-flux ($dT/dr = 0$) condition is also imposed at this boundary. At the outer boundary a geometrically thin Keplerian disc is assumed.

The method used in this work is a time-dependent method. The initial conditions arc the superposition of an isothermal atmosphere and an inflowing disc of matter.

The viscosity prescription used here is based on the approach developed by Godon (I 995c), and is similar to the one used in Godon (1995b). The value of the viscosity parameter is $\alpha \approx 0.1$ (more precisely $0.05 < \alpha < 0.15$). This ensures solutions with a distinct thermal boundary layer and subsonic radial infall velocities (see also sec. 2.3, and Godon 1 Mm).

2.'2 The numerical method

The spatial dependence of the equations is treated with the use of a Chebyshev spectral method (Gottlieb & Orszag 1977; Voigt, Gottlieb & Hussaini 1 984; Canutto et al. 1988), while the time dependence of the equations is solved with an implicit Crank-Nicholson scheme for the energy equation and an explicit second order 1 Runge-Kut t a method for the remaining equations. A time dependent Chebyshev pseudospectral method of collocation has been developed recently to treat astrophysical flows (Godon & Shaviv 1993), and has been applied to one-dimensional accretion disc boundary layers (Godon 1995a & b, Godon et al. 1995) and two-dimensional rotating envelops of stars (Godon & Shaviv 1995). All the details of the numerical method can be found in the references above. In the present calculations 64 grid points (the collocation points) are chosen to ensure good resolution and stability of the numerical scheme.

2.3 Boundary layers modeling

Accretion disc boundary layers have been modeled using the above time dependent method to treat boundary layers around white dwarfs (in Cataclysmic Variable systems, Godon 1995a; Godon et al. 1995) and pre-main sequence stars (T-Tauri and FU Orionis stars, Godon 1995 b). In these calculations the energy dissipated in the dynamical boundary layer (region over which the angular velocity in the inner part of the disc decreases from its Keplerian value to adjust to the slowly rotating stellar surface) is radiated radially outward and heats up a much wider region (the t hermal bou ndary layer, region over which the temperature is significantly larger than the disc temperature). The boundary layer energy is therefore emitted from a rat her broad region, and the temperature is consequentl y rather low.

Around white dwarfs the dynamical boundary layer, obtained in the above calculations, has a width $\delta_{BL}^{dyn} \approx 10^{-3} R_*$, a thermal boundary layer width $\delta_{BL}^{Th} \approx$ 0.1 R* and an effective temperature $T_{eff} \approx 10^5 K$, for a mass accretion rate $\dot{M} \approx 10^{-9} M_\odot/y$. For pre-main sequence stars the picture is completely different. One obtains $\delta_{BL}^{dyn} \approx 0.1 - 0.5 R_*$, $\delta_{BL}^{Th} \approx$ 0.3-- Ill*, $T_{eff} \approx$ 7000-- 12000K, for $\dot{M} = 5 \times 10^{-7}$ up to 10--4M~)/y. For accretion around main sequence stars (symbiotic stars with $M \approx 1$-- 10 x $10^{-5} M_\odot/y$) one expects boundary layers widths similar to the case of pre-main sequence stars but with temperature similar to the white dwarf case (Mikołajewska 1995).

However, one must take into consideration that some of the physical assumptions, which are still a subject of debates, can affect the numerical results (for example the viscosity parameter α). Therefore, we justify below in some details the assumptions made in the present work.

- An inner boundary condition is needed on one of the thermodynamic variables (the density, the pressure, the energy or the temperature). The boundary condition is generally imposed on the temperature or on the radial flux of energy $F_r = \sigma T_{*eff}^4$ (where T_{*eff} is the

effective temperature of the star). The temperature boundary condition leads to solutions in which the boundary layer pours energy into the star, while the flux boundary condition leads to solutions in which the star pours energy into the boundary layer. The temperature condition is difficult to treat numerically, since it can lead to a large temperature gradient near the stellar surface. The flux boundary condition leads to higher boundary layer temperatures than the temperature condition. This is especially true for low mass accretion rate systems (like in T Tauri, Regev & Bertout 1995, Godon et al. 1995, and Godon 1995b). Fortunately, at higher accretion rates, the results do not depend on the boundary condition (Godon 1995b). Therefore, we decide to impose a non-flux condition $dT/dr = 0$ at the inner boundary, which has the advantage of being easy to treat numerically. For the mass accretion rates considered in the present work, the three different boundary conditions (flux, temperature and non-flux) lead to practically the same results.

The value of the alpha viscosity parameter, as well, can significantly affect the solutions. When a low value of α is assumed ($\approx 10^{-4}$ - 10^{-3}), a much larger density is needed to reproduce a given mass accretion rate in comparison to the case where $\alpha \approx 0.1 - 1$. Furthermore, the density affects the opacity law, the diffusion and advection of energy. In pre-main sequence accretion discs this effect is dominant: when $\alpha < \alpha_{critic} \approx$ few 10^{-2}, the solutions exhibit no distinct the thermal boundary layers, and the maximum effective temperature is rather low (Godon 1995b). In fact, a very low α has been justified only in FU Orionis discs, to reproduce the outburst time scales ($\alpha = 10^{-3} - 10^{-4}$). On the other hand, a large α (≈ 1) leads to supersonic radial infall velocities, in contradiction with the causality formalism developed by Popham & Narayan 1992. Consequently, we chose an intermediate value for the viscosity parameter $\alpha \approx 0.1$. Solutions obtained with $\alpha \approx 0.1$ have subsonic radial infall velocities and higher boundary layer temperatures.

In all the boundary layers calculations we performed previously, as well as in the present calculations, there are mainly three characteristic time scales involved in the evolution of the models: the dynamic time $\tau_d \approx 2\pi/\Omega_K$, the viscous time $\tau_v \approx R_*/v_r$, and the time scale over which a perturbation propagates in the inner part of the disc $\tau_p \approx R_*/c_s$ (in the present calculations $\tau_p < \tau_d < \tau_v$). As the models evolve from the initial conditions, strong perturbations appear and then decay on a time $\sqrt{\tau_p \tau_v}$. At this stage, most of the variables are already close to their steady state values, however the decreasing luminosity is still much larger than L_{acc}. Large amplitude oscillations (local variation of $\dot{M}$) propagates between the boundaries. After a time $\tau_s \approx \sqrt{\tau_v \tau_d}$ the luminosity of the model approaches $L_{acc}/2$, while all the other variables (including the temperature) do not change appreciably (few percent at most), and the amplitude of the oscillations have decreased by about 50 percent (see Godon 1995a & b, for more details). All the models in this work have been followed on a time scale τ_s to ensure that the results are close to their steady state value.

3. HOT 1301JN1)AR% LAYERS AROUND AX PER ANI) CI CYG

In this section we present the results of several models of accretion disc boundary layers around main sequence stars corresponding to the symbiotic binaries AX Per and CI

Cyg. The results are summarized in 'l'able 1. In column 1 the names of the models are listed. The input parameter of the models are the radius of the accreting star (column 3), the mass of the accreting star (column 2), and the mass accretion rate (column 4). The important output parameters are the thickness of the inner part of the disc (column 5), the width of the thermal boundary layer (column 6), the width of the dynamic boundary layer (column 7), and the maximum effective temperature in the thermal boundary layer region (column 8). The models are grouped in three sets. In the first set (models 1,5,31, and 2) the mass of the star is kept constant while the radius varies from 0.2 to 0.4 solar radius (for a mass accretion r-ate of a few 10^{-5} solar mass per year). In the second set (models 3,31,2,22,23,24, and 4) the radius and the mass of the accreting star are kept constant while the mass accretion rate is increased from 1 x 10^{-5} to 3 x 10--4 solar mass per year. In the last set (models 5,6,7, and 8) the stellar radius is kept constant while the mass of t he star varies for different mass accret ion rates.

A look at the table (first and last sets) immediately shows that temperatures of $T > 10^5$ K are reached only for $M_* = 0.5 M_\odot$ and $R_* = 0.2 R_\odot$.

The seven models of the second sets (models 3,31 ,2,22,23,?.4, and 4 in table 1) are drawn in figure 1. This graphs shows the dependence of the maximum effective temperature as a function of the mass accretion rate for $M_* = 0.5 M_\odot$ and $R_* = 0.2 R_\odot$. The maximum effective temperat ure (in the boundary 1 ayer region) increases with increasing mass accretion rates. It reaches a maximum of 136 x 10^3K for $M = 7 \times 10^{-5} M_\odot/y$, then it stays nearly constant ($T \approx 1.3 \times 10^5 K$) as the mass accretion rate exceeds 10--4 solar mass per year. In figures 2a-c we show the temperature profile, the vertical thickness, and the angular rotation rate for model 3. The same parameters are shown in figure 3a- c for model 2'2, when the temperature reaches its maximum. It must be stressed that the radial scale is not the same in figures 2 and figures 3. As the mass accretion rate increases and the temperature reaches a maximum, the thickness of the disc increases from ≈ 0.1 up to $\approx 0.35 R_*$, and both the thermal and dynamical boundary layers increase by about the same factor.

4. DISCUSSION AND CONCLUSION

The symbiotic binaries AX Per and Cl Cyg have several observational characteristics in common. They are both transferring material at a few × 10--s~4~ $/y$ into an accretion disc around a main-sequence stars of mass $M_* \approx 0.4 - 0.5 A1_{0)}$ and radius 0.2-- $0.4 R_\odot$. The optical luminosity increases by two orders of magnitude from quiescence to outburst, while the H el 1 emission lines present during quiescence are not observed during outburst. This indicates that the effective temperature of the not component drops from $T \approx 10^5 K$ in quiescence to $T < 60,000 K$ during outburst (Kenyon et al. 1991; Kenyon & Mikołajewska 1992).

In the present calculations we found out that the boundary layer can reach a, temperature above $10^5 K$, assuming for the accreting star a mass $M_* = 0.5 M_\odot$ and a radius

$R_* = 0.21$?... These values are in fairly good agreement with the first estimates of Kenyon et al. (1 991) and Kenyon & Mikołajewska (1 992).

Furthermore, we obtained that the maximum effective temperature of the models initially follows the increase of the mass accretion rate, but it stops to do so as the mass accretion rate approaches 10--4 solar mass per year. A similar standstill in the effective temperature, for similar values of $\dot{M}$, was obtained for discs around pre-main sequence stars (Popham et al. 1993). This result was believed to be due to both an increase in the boundary layer width and a larger stellar radius at high accretion rates (Popham et al. 1993). In our calculations the high accretion mass models and the low accretion mass models were all computed with the same radius. In order to see the effect of the radius on the temperature, one has to consider TaMc 1. The first set of results in Table 1 (models 1,5,31 and 2) show that the maximum effective temperature is roughly proportional to 1 /ii?,. Clearly, in order to fit the observations, one has to increase the radius of the accreting star by a factor of 2-3 during outburst. The lack of increase in the effective temperature is not sufficient to explain the observations.

An additional factor which should be taken into consideration is the cooling due to the vertical expansion of the disc, which is not fully taken into account in the calculations, since the equations are not solved in the vertical direction but only integrated vertically.

However, more physical insight can be obtained by comparing the boundary layer luminosity and the accretion luminosity. Assuming a geometrically thin disc, the boundary layer luminosity can be given by (Kluzniak 1987): $L_{bl}^{th} = (1 - \Omega_*/\Omega_{K*})^2 L_{acc}/2$, where Ω_* is the angular rotation rate at the outer stellar envelop, Ω_{K*} is the Keplerian angular velocity at one stellar radius and $L_{acc} = GM_* \dot{M}/R_*$ is the accretion luminosity. In the present case, this is a rough approximation, since the high accretion models have $H/r \approx 0.4$ and a boundary layer of large radial extent. A comparison between the expected boundary layer luminosity L_{bl}^{th} and the luminosity obtained from the calculations $L_{bl}^{c} = \int 2\pi r F_z dr$, shows that at high accretion mass rates L_{bl}^{c} is significantly smaller than L_{bl}^{th}. Since a nom flux boundary condition is used at the inner edge of the boundary layer, this energy is advected across the inner boundary. The advected 'flux' of energy is $F_{adv} = v_r \rho \epsilon$, where $\rho\epsilon = 3\mathcal{R}\rho T/2\mu + aT^4$. In table 2 we show the rate of energy which is advected across the inner boundary $L_{adv} = 2\pi r 2H F_{adv}$, the expected boundary luminosity L_{bl}^{th} and the boundary layer luminosity L_{bl}^{c} obtained in the calculations for the high accretion mass rate models (23, 24 and 4, models for which L_{bl}^{c} is significantly lower than L_{bl}^{th}). For $\dot{M} \geq$ 10--4 $M_\odot/y$, more than 30 percent of the energy dissipated in the boundary layer region is advected into the inner boundary, and only 2/3 is radiated vertically (similar results were obtained for accretion discs around pre-main sequence stars with M $\approx 10^{-4} M_\odot/y$ in Godon 1995 b). In figure 4 we have drawn the advective flux of energy F_{adv} (thick line) and the radiative flux of energy F_r (dotted line) in the inner part of the disc for model '24. The energy dissipated in the dynamical boundary layer region is radiated outward ($F_r > 0$, since the mid-plane temperature T_c decreases monotonously outward) and is

responsible for the formation of a thermal boundary ayer of large radial extent and low temperature. The energy advected inward is about 30 percent of the energy radiated radially outward. The inner part of the disc is therefor c partially dominated by advection. In fact as expected in advection-domin ated discs (Narayan & Yi 1994), the inner part of the disc is sub-Keplerian and H/r is of the order of one.

Our one-dimensional zqqn-each must be considered as a very rough approximation when M ≈ 10–4 $M_\odot$ /y. In fact, advect ive accretion flows arc quasi-spherical (Begelman & Meier 1982), and a two-dimensional approach mighit be needed to resolve the accretion problem. In addition, the accretion reaches the Eddington limit. Assuming an electron scat tering opacity and a solar composition for the accretion flow leads to $L_{acc}/L_{Edd} \approx$ **800 x** $\dot{M}(M_\odot/y)(R_*/R_\odot)^{-1}$. With a stellar radius of $0.2R_\odot$, the Eddington limit for the mass accretion rate becomes $\dot{M}_{Edd} \approx$ 2.6 X 10--4 $M_\odot y$" . Again, in this limit the flow is quasi-spherical (Begelman & Meier 1982). Moreover, the fate of the advected energy is not clear. An interesting issue, however, is one in which the advected energy would change the equilibrium of the accreting star and induce an increase of the stellar radius (or at least an increase of the outer envelop of the star). As the mass accretion rate increases from M $\approx 10^{-5} M_\odot/y$ up to 3 x $10^{-4} M_\odot/y$, the energy gained by the star through accretion increases from $\zeta = L_{adv}/L_{acc} \approx 0.001$ up to $\zeta \approx$ ***0.12.*** Evolutionary calculations of accreting stars (Prialnik & Livio 1985) show that a $0.5M_\odot$ star with a deep convective envelop is proned to increase its radius after it has accreted a few **X 10-4** $M_\odot$ and when $\zeta >$ **0.05** and $M > 10^{-6} M_\odot/y$. The increase of the stellar radius could explain the dramatic fall of the temperature of the inner part of the disc (models 1,5,31 and 2 in Table 1), however the temperature and the luminosity of the accreting star arc also increasing significantly as the radius increases.

Advective flows are also susceptible to produce outflows (Narayan & Yi 1994), which could interact with the accretion disc. Obviously, t he physics involved in advective flows is attractive since it seems that it could help to understand the behaviour of outburst in symbiotic binaries, but it is far beyond the scope of the present one-dimensional calculations.

ACKNOWLEDGEMENTS

1 thank Joanna Mikołajewska for helpful discussions on symbiotic stars and for providing me with a reprint of her paper. I am also thankful to David Meier for comments and discussions. I thank the Referee for his remarks and corrections which led to an improved version of the paper. The Cray Super computer (JPL/Caltech Cray Y-MP2E/232) used in this investigation was provided by funding from t he NASA Offices of M ission to Planet Earth, Aeronautics, and Space Science. This work was performed while the author held a National Research Council - (NASA Jet Prepulsion Laboratory) Research Associateship. This research was carried out at the J et Propulsion Laboratory, California Institute of Technology, under contract, to the National Aeronautics and Space Administration.

REFERENCES

Begelman, M. C., & Meier, D. L. 1982, ApJ, 253, 873

Canuto, C., Hussaini, M. Y., Quarteroni, A., & Zang, T. A. 1988, Spectral Methods in Fluid Dynamics (Springer Verlag, New-York)

Godon, P. 1995a, MNRAS, 274, 61

Godon, P. 1995b, MNRAS, in press

Godon, P. 1995c, MNRAS, in press

Godon, P., Regev, O., & Shaviv, G. 1995, MNRAS, 275, 1093

Godon, P., & Shaviv, G. 1993, Com~mt.Methods Appl.Mech.Engrg., 110, 171

Godon, P., & Shaviv, G. 1995, ApJ, 447, 797

Gottlieb, l)., & Orszag, S. A. 1977, Numerical Analysis of Spectral Methods: Theory and Applications, NSF-CBMS Monograph n.26, Soc.Ind. and Appl.Math., Philadelphia PA

Kenyon, S. J., & Hartmann, 1,.1990, ApJ, 349, 197

Kenyon, S. J., Oliversen, N. A., Mikołajewska, J., Mikołajewski, M., Stencel, R. E., Garcia, M. R., & Anderson, C. M. 1991, AJ, 101, 637

Kluzniak, W. 1987, Ph.D. Thesis, Standford University

Lioure, A., & Le Contel, O. 1994, A & A, 285, 185

Mikołajewska, J. 1995, private communication

Mikołajewska, J., & Kenyon, S. J. 1992, AJ, 103, 579

Narayan, R., & Yi, 1.1994, ApJ, 428, L13

Popham, R., Narayan, R. 1992, ApJ, 394, 255

Popham, Il., Narayan, R., Hartmann, I,., & Kenyon, S. 1993, ApJ, 415, L127

Popham, R., & Narayan, R. 1995, ApJ, 442, 337

Prialnik, D., & Livio, M. 1985, MNRAS, 216, 37

Pringle, J. E. 1977, MNRAS, 178, 195

Regev, O., & k-tout, C. 1995, MNRAS, 272, 71

Shakura, N. I., & Sunyaev, R. A. 1973. A & A, 24, 337

Voigt, R. G., Gottlieb, D., & Hussaini, M. Y. 1984, Spectral Methods for Partial Differential Equations, (SIAM-CBMS, Philadelphia)

FIGURE LEGENDS

Figure 1.. The maximum effective temperature reached in the boundary layer region as a function of the mass accretion rate. The temperature is given in units of $10^3 K$, and the mass accretion rate is in $log(M_\odot/y)$. The accreting star has a mass of $M_* = 0.5 M_\odot$ and a radius $R_* = 0.2 R_\odot$. The temperature initially tracks the increase of mass accretion rate, but it slightly drops close to the maximum.

Figure 2a. The effective temperature (in Kelvin) in the inner part of the disc is drawn as a function of the radius (in units of R_*), for model 3 (see table 1).

Figure 2b. The vertical thickness of the disc H/r is drawn as a function of the radius, for model 3.

Figure 2c. The angular velocity $\Omega(r)/\Omega_K(r)$ is drawn as a function of the radius, for model 3.

Figure 3a. The effective temperature in the inner part of the disc for model 22.

Figure 3b. The vertical thickness fo the disc H/r for model 22.

Figure 3c. The angular velocity for model 22.

Figure 4. The advective 'flux' of energy (full line) and the radiative flux of energy (dotted-line) are drawn as a function of the radius (in units of R_*) for model 24. One third of the energy dissipated in the dynamical boundary layer is advected into the inner boundary and only 2/3 contributes to the boundary layer luminosity.

TABLE 1

BOUNDARY LAYER MODELS FOR SYMBIOTIC BINARIES

[1] model	[2] M_* ($M_\odot$)	[3] R_* ($R_\odot$)	[4] $\dot{M}$ ($M_\odot/y$)	[5] [a] H (R_*)	[6] δ_{BL}^{Th} (R_*)	[7] δ_{BL}^{dyn} (R.)	[8] T_{eff}^{Max} (10^3K)
1	0.5	0.4	2.0×10^{-5}	0.17	0.30	0.10	Go
5	0.5	0.3	4.0×10-5	0.240.16	0.35	0.15	97
31	0.5	0.2	2.5×10^{5}	0.25.0.16	0.50	0.10	120
2	0.5	0.2	4.0×10^{-5}	0.300.20	0.7(1	0.20	130
3	0.5	0.2	1. OX1O-5	0.15.0.12	0.40	0.05	100
31	0.5	0.2	2.5 x 10-5	0.25-11.16	0.50	0.10	120
2	0 . 5	0.2	4.0×10^{-5}	0.30-0.20	0.70	0.20	130
22	0.5	0.2	7.0×10^{-5}	0.35-(1.20	1.00	0.20	136
23	0.5	0.2	9.0×10"5	0.26 (1.20	0.70	0.20	126
24	0.5	0.2	1.8×10^{-4}	0.37-0.23	0.70	0.40	135
4	0.5	0.2	3.0 x 10-4	0.40-0.25	0.70	0.50	135
5	0.5	0.3	4.0×10^{-5}	0.24-0.16	0.35	0.15	97
6	0.4	0.3	7.0×10^{-5}	0.26-0.20	0.50	0.15	88
8	0.3	0.3	2.0×10^{-5}	0.18	0.40	0.10	69
7	0.3	0.3	2.0×10-4	0.40-0.25	1.00	0.40	94

*In column 5, the first value correponds to H in the boundary layer region, the second refers to the region of the disc directly adjacent to the boundary layer.

TABLE 2

ADVECTIVE BOUNDARY LAYERS IN SYMBIOTIC BINARIES

[1] model	[2] $\dot{M}$ ($M_\odot/y$)	[3] L_{acc} (10^{36}erg)	[4] L_{bl}^{th} (10^{36}erg)	[5] L_{bl}^{c} (10^{36}erg)	[6] L_{adv} (10^{36}erg)
23	9.0×10^{-5}	14.1	5.9	4.7	1.
24	1.8×10^{-4}	27	10.9	7.4	3.
4	3.0×10^{-4}	45.3	18.4	12.4	5.6

Figure 1.

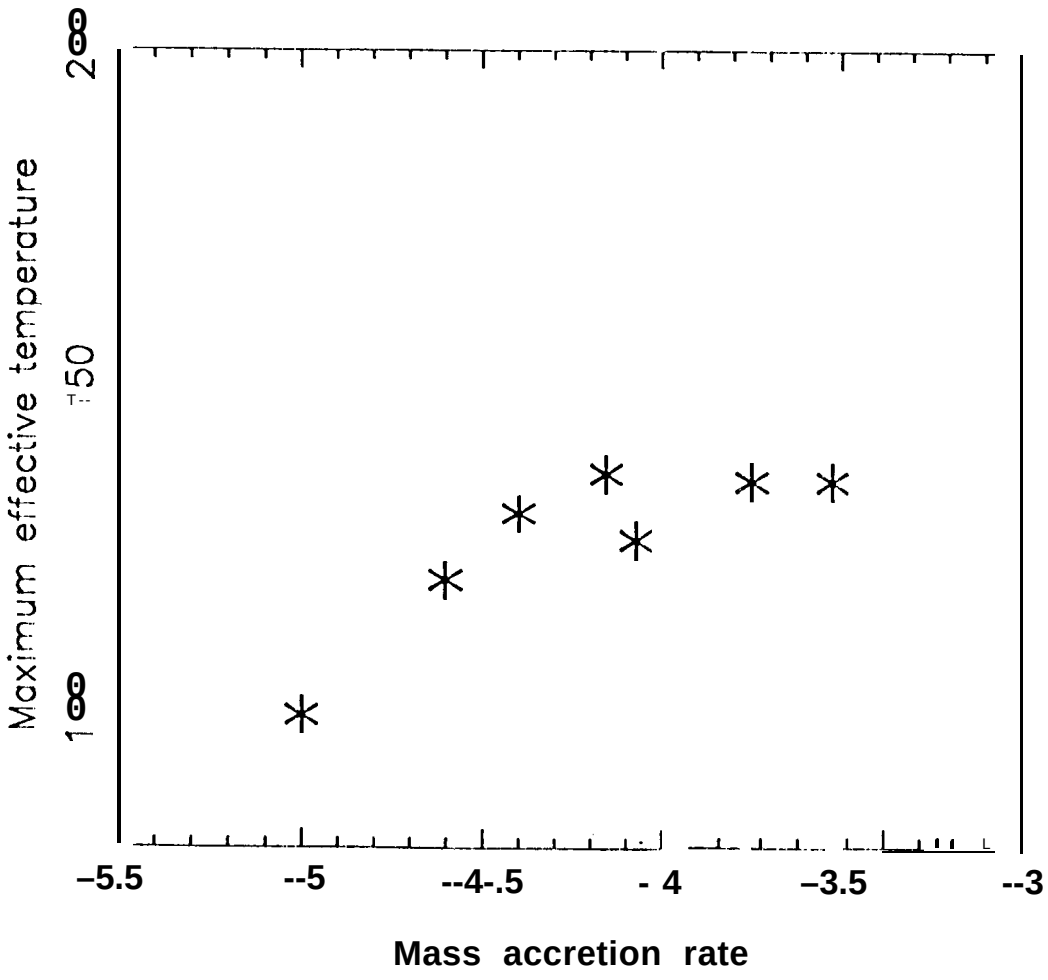
Maximum effective temperature
200
150
100
–5.5
--5
--4-.5
- 4
–3.5
--3
Mass accretion rate

Figure 2a.

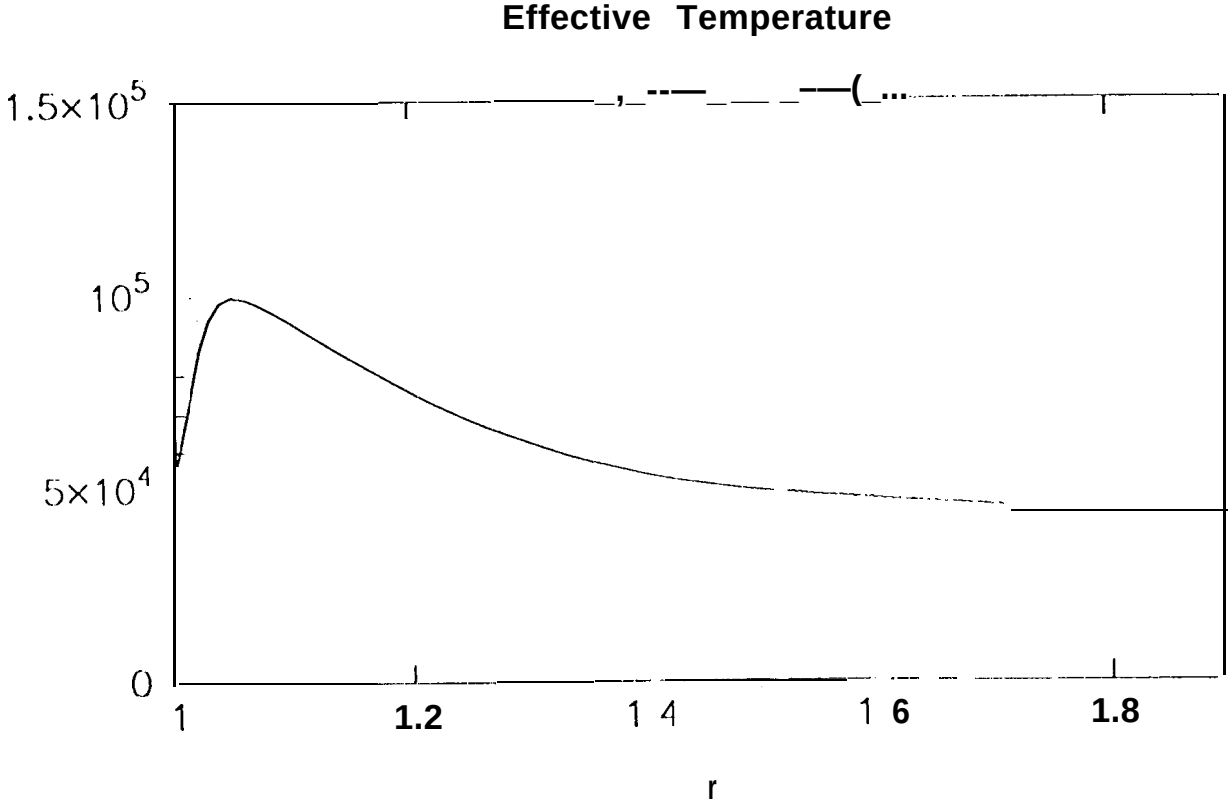

Figure 2b.

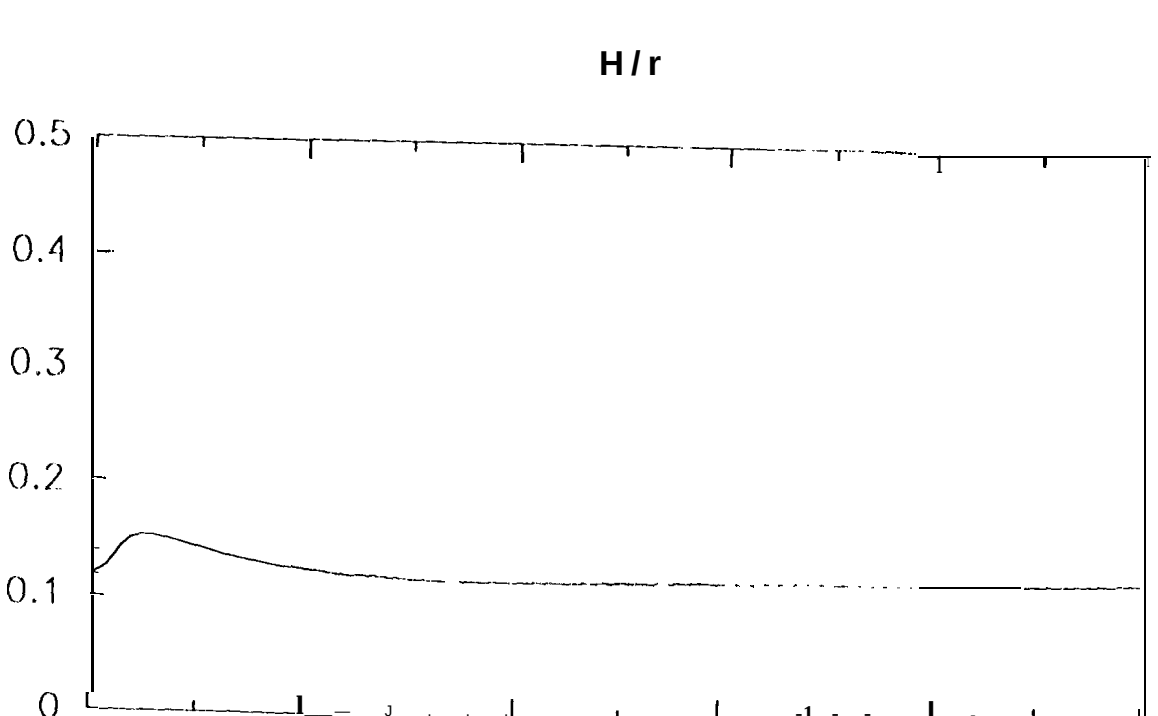

Figure 2c.

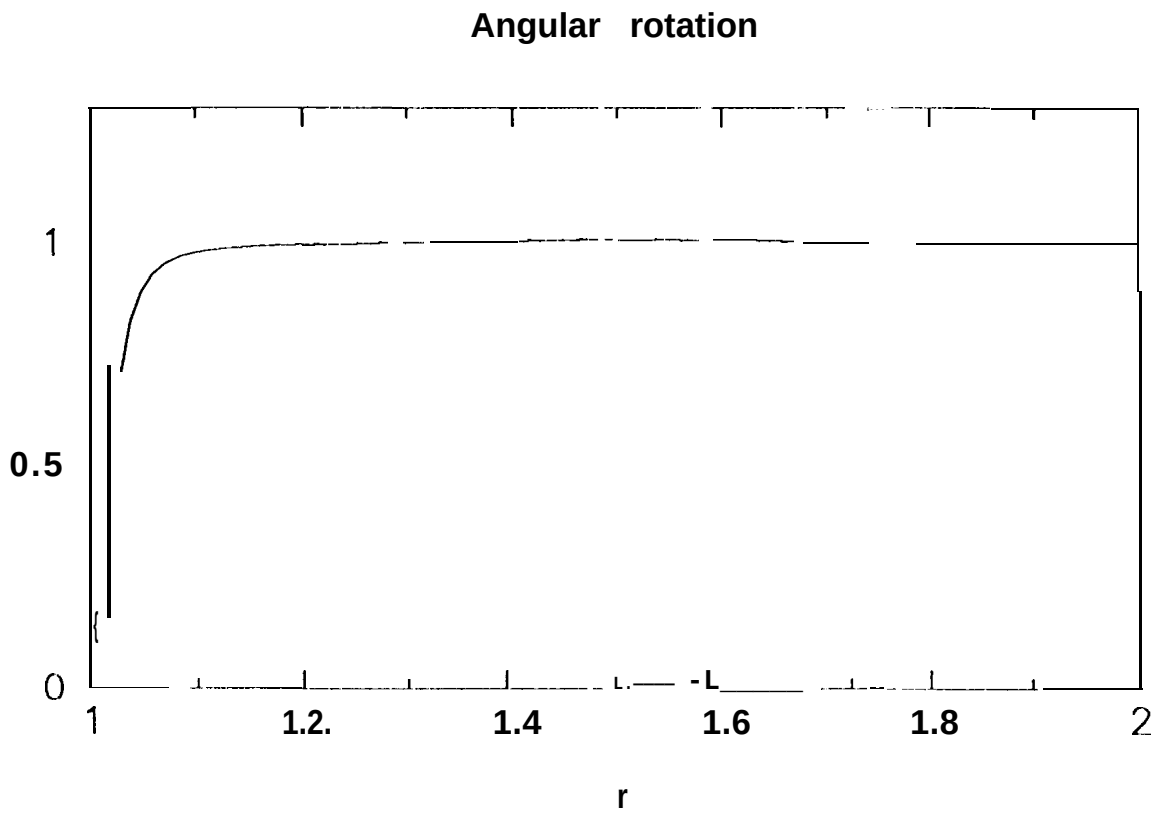

Figure 3a.

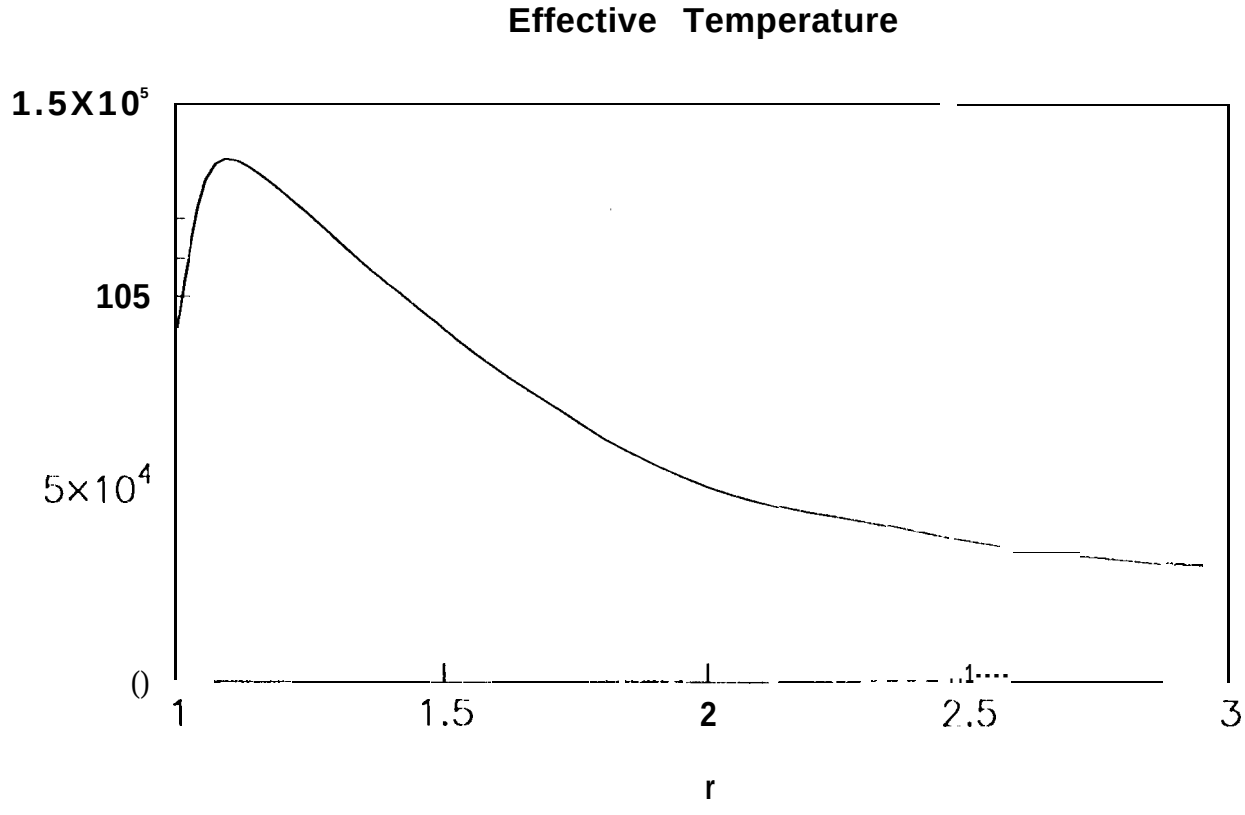

Figure 3b.

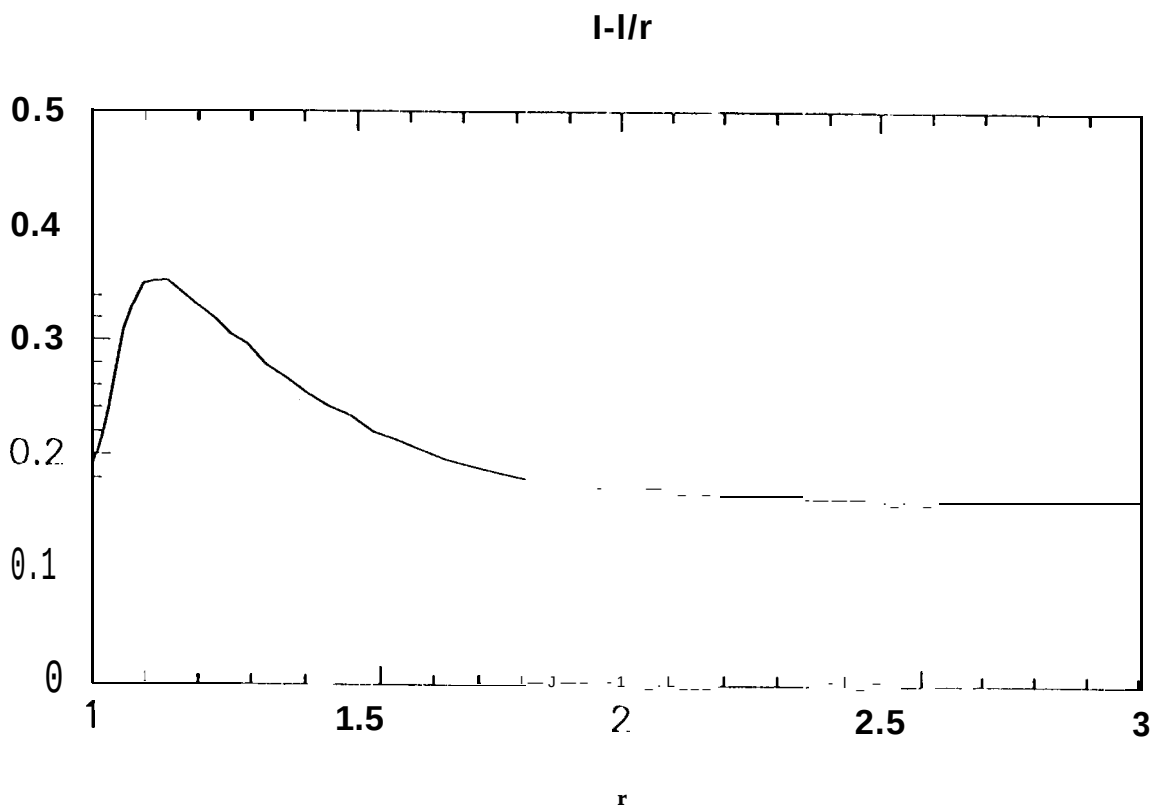

Figure 3c.

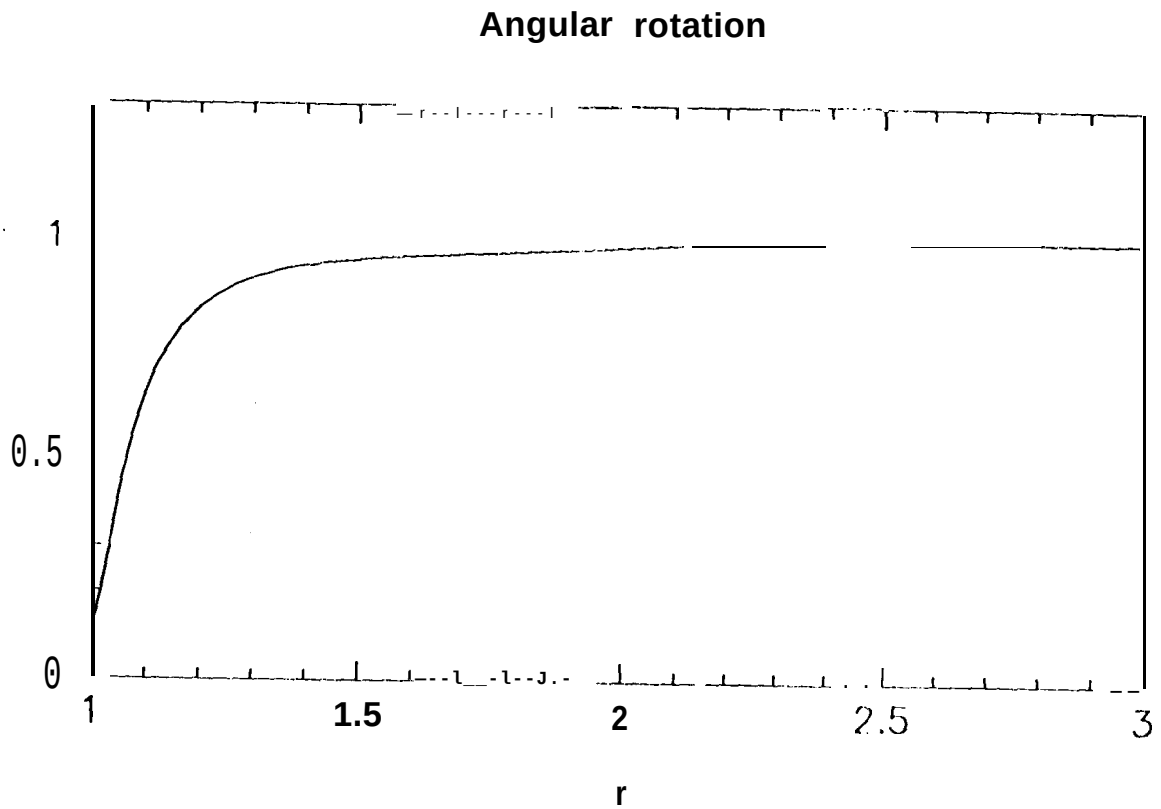

Figure 4.

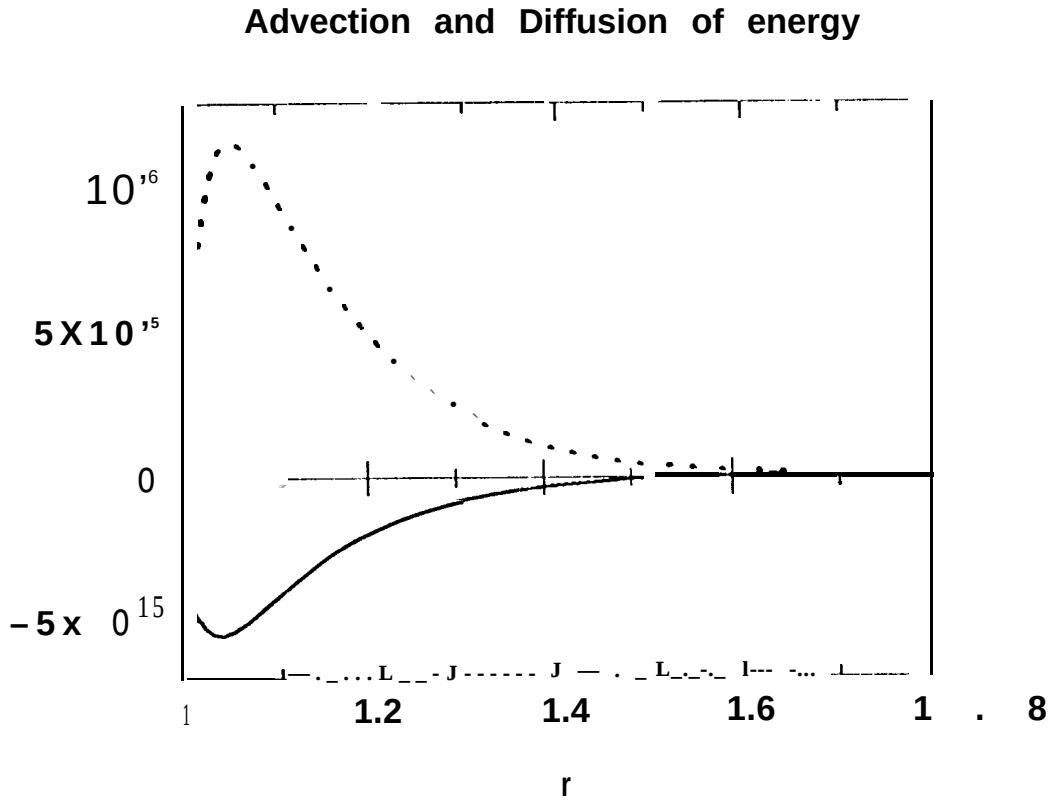
Advection and Diffusion of energy
10'6
5X10'5
0
-5x 0 15
1
1.2
1.4
1.6
1 . 8
r